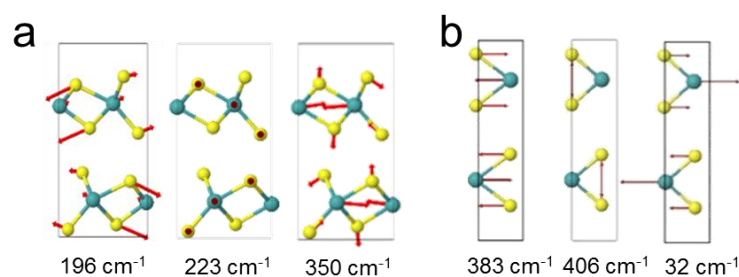
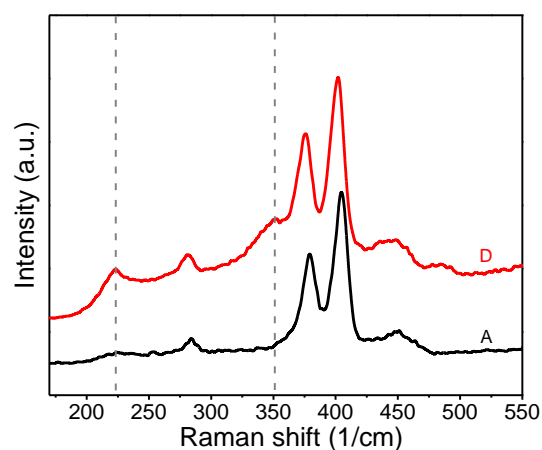


**Fig. S1** Detailed experimental set-up for lithium electrochemical intercalation process of five different button cells, with MoS<sub>2</sub> acting as cathode and lithium plate as anode respectively.



**Fig. S2** The Raman vibrational diagrams of dT- (a) and 2H-MoS<sub>2</sub> (b) respectively. The three peaks located at 196, 223, 350 cm<sup>-1</sup> in (a) are the Raman peaks of dT-MoS<sub>2</sub>, while the peaks at 383, 406 and 32 cm<sup>-1</sup> in (b) are the Raman peaks of 2H-MoS<sub>2</sub>.



**Fig. S3** Raman fingerprints of pristine MoS<sub>2</sub> powder and complete lithium intercalated MoS<sub>2</sub> with discharge potential at 0.9 V by 457 nm excitation laser. The two peaks located at 223, 350 cm<sup>-1</sup> (marked with dashed lines) are the Raman feature peaks of dT MoS<sub>2</sub>.

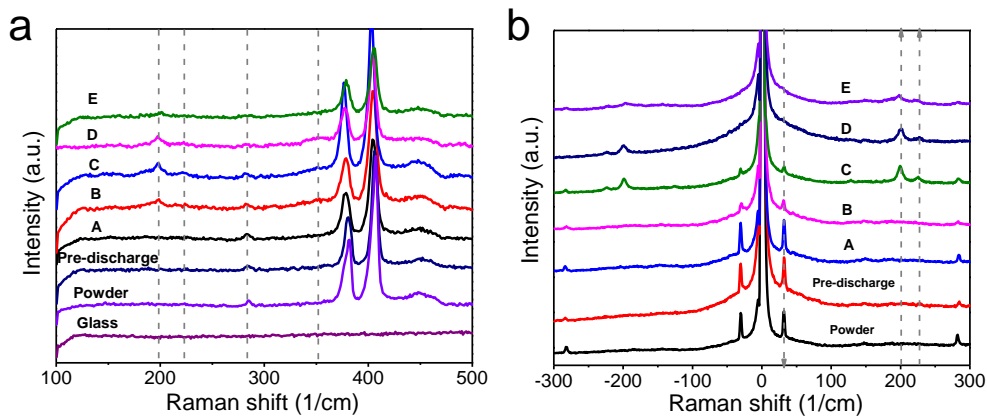


**Fig. S4** High frequency (a) and ULF (b) Raman spectra of pristine  $\text{MoS}_2$  powder and withdrawn  $\text{MoS}_2$  cathodes in Figure 1a after ultrasonication and centrifugation four times.

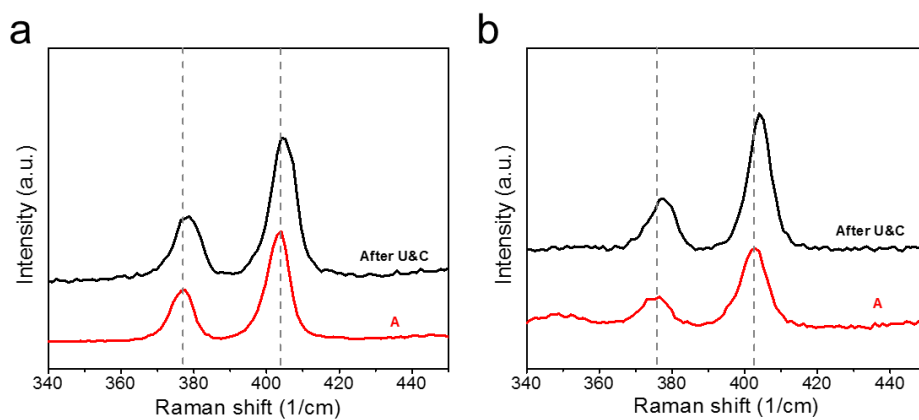


**Fig. S5** Raman spectra comparison respecting  $E_{2g}^1$  and  $A_{1g}$  modes between the just withdrawn  $\text{MoS}_2$  cathodes after being washed and the one after ultrasonication and centrifugation four times.

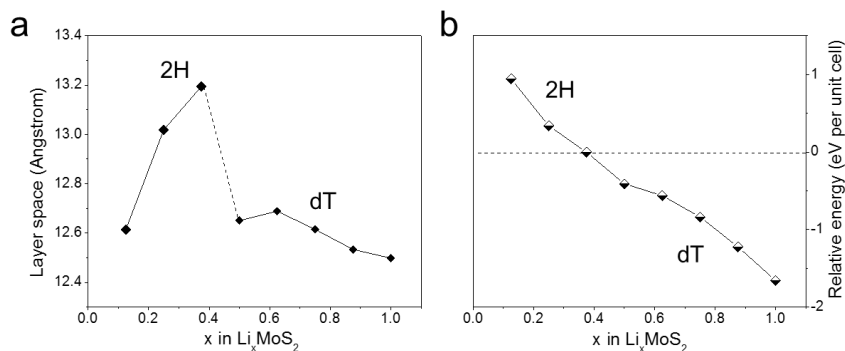


**Fig. S6** Layer space evolution (a) and relative energy per unit cell (b) in  $\text{Li}_x\text{MoS}_2$  with different  $\text{Li}^+$  concentrations by the first-principles calculations.

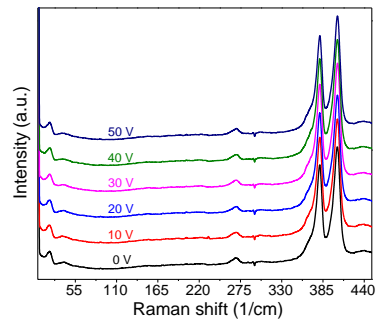


**Fig. S7** Raman spectra of bilayer 2H-MoS<sub>2</sub> with applied gate voltages at 10 V, 20 V, 30 V, 40 V and 50 V respectively.

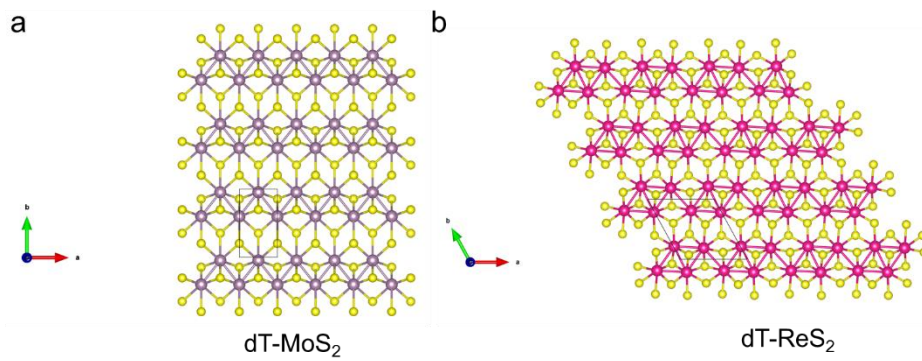


**Fig. S8** Atomic structures of the top views for dT-MoS<sub>2</sub> and ReS<sub>2</sub> monolayer.